X-Ray Scattering from Sodium-Doped Polyacetylene: Incommensurate-Commensurate and Order-Disorder Transformations

M. Winokur, Y. B. Moon, and A. J. Heeger
Institute for Polymers and Organic Solids, University of California, Santa Barbara, Santa Barbara, California 93106

J. Barker and D. C. Bott
British Petroleum Research Centre, Sunbury-on-Thames, England

and

H. Shirakawa
Institute for Materials Science, University of Tsukuba, Ibaraki 305, Japan
(Received 8 December 1986)

X-ray scattering carried out *in situ* during electrochemical doping indicates an unusual sequence of structural transitions. On doping to ≈ 6–7 mole%, lightly doped regions coexist with a discommensurate-domain channel structure. As the Na concentration increases, the density of domain walls decreases. When the discommensuration density falls to zero, the Na channels form a commensurate $\sqrt{3}\times\sqrt{3}$ superlattice with respect to the (average) triangular lattice of $(CH)_x$ chains. At still higher concentrations, the Na lattice becomes unstable and transforms into a disordered "fluid" phase within the ordered polyacetylene structure.

PACS numbers: 64.70.Kb, 64.70.Rh

Reversible doping of conducting polymers involves charge storage in the π-electron system and insertion of counter ions into the structure. As a result, doping leads to rearrangement of the polymer chains and to formation of new ordered structures. Identification of these structures and their evolution during doping is fundamentally important, for the electronic properties are determined by the structure.

In this Letter, we present the initial results from x-ray scattering experiments carried out on sodium-doped polyacetylene $[(Na^+)_y(CH)^{-y}]_x$ *in situ* during electrochemical doping. The data indicate an unusual sequence of reversible transitions within a channel structure in which the local unit is a column of Na ions surrounded by three $(CH)_x$ chains. Although structural results have been reported for polyacetylene (PA) doped with alkali metals[1] or various electron acceptors,[2] this is the first *in situ* study; the ability to monitor the scattering data continuously has made it possible for us to characterize the full series of transformations. (i) At low y, the Na channels form a strongly modulated incommensurate lattice in the plane normal to the polymer chains within the PA host. Below 6 mole%, this incommensurate lattice coexists as a two-phase mixture with lightly (random) doped PA. (ii) At intermediate y (≈ 10 mole%), the Na lattice becomes commensurate forming a $\sqrt{3}\times\sqrt{3}$ superlattice relative to the average triangular spacing of the *rearranged* $(CH)_x$ chains. (iii) At higher y (>10 mole%), the Na superlattice transforms into a dense disordered state best characterized as a highly modulated fluid.

These features represent an unusual example of two interpenetrating mass-density waves with continuously varying periodicities; the strong interaction between the two results in the formation of a novel discommensuration-domain channel structure.

Electrochemical cells consisted of the polymer sample ($\simeq 0.4\times 3\times 3$ mm^3, wrapped with 30-μm Ni wire), sodium metal counterelectrode, and electrolyte (0.2 M solution of $NaB\Phi_4$ in 2-methyltetrahydrofuran), all inside a 3.5-mm glass capillary deformed to minimize solvent scattering volume. The counterelectrode was separated from the $(CH)_x$ sample and was out of the x-ray beam. Stretch-oriented *trans*-$(CH)_x$ samples were used, prepared via the Durham route[3] or by the Shirakawa process.[4] Uniaxial stretching orients the material along the c axis (the polymer backbone direction); directions normal to the c axis are polycrystalline with ≈ 100 Å coherence length. The mosaic spreads are $\approx 35°$ and $\approx 10°$ for the Shirakawa and Durham samples, respectively. The electrochemical cells were mounted on a diffractometer equipped with a 1.5-kW copper x-ray source fitted with a graphite monochromator. The PA samples were typically doped for periods of 12 h at currents of less than 5 μA and then allowed to reach equilibrium for 12 h. Drift of the open-circuit voltage (V_{oc}) during the relaxation period was usually within 150 mV of the set-point voltage. A complete doping cycle required about four weeks. With respect to V_{oc} the evolution of structure can be subdivided into three major regions; from 1600 to 800 mV, from 800 to 400 mV, and finally 400 mV and below. These ranges have been calibrated by electrochemical voltage spectroscopy.[5]

Figure 1 shows a series of $(hk0)$ scans obtained from a Shirakawa *trans*-$(CH)_x$ sample on doping from 0 to ≈ 6 mole% (820 mV) Na. The inset shows the PA

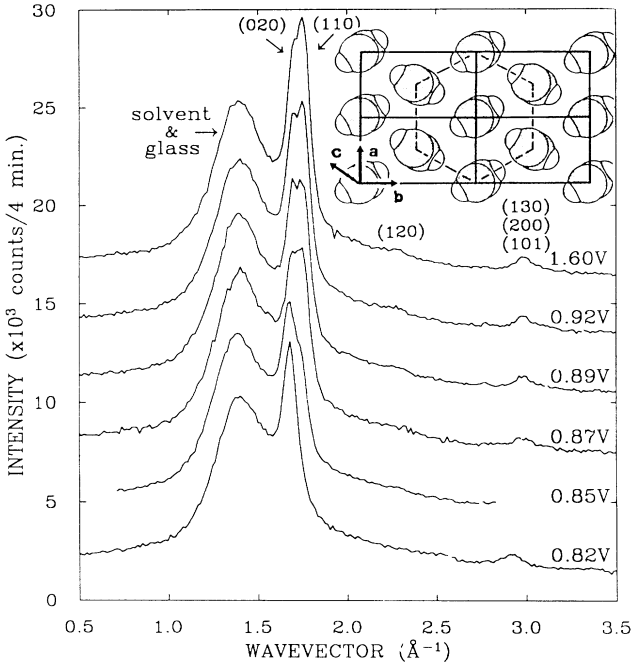

FIG. 1. Equatorial ($hk0$) scans for Na-doped oriented Shirakawa PA from 0 to ≈ 6 mole% (V_{oc} from 1.6 to 0.82 V). Inset: "Top view" of neutral PA showing the hidden hexagonal symmetry.

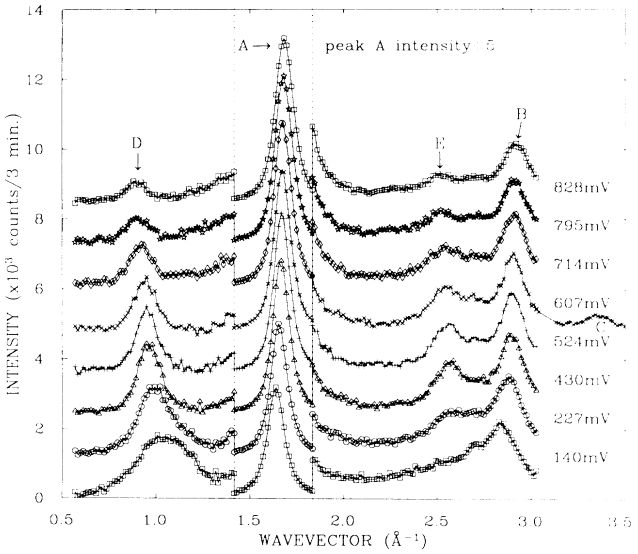

FIG. 2. Equatorial ($hk0$) scans showing the structural evolution of oriented Durham PA on Na doping from ≈ 6 to ≈ 14 mole% (V_{oc} from 828 to 140 mV).

structure in a plane perpendicular to the polymer chains; note the hidden hexagonal symmetry of the polymer chains. For the highest cell voltage (very dilute doping), we identify peaks corresponding to crystalline regions of neutral *trans*-$(CH)_x$ superimposed on an amorphous background (from the solvent, glass, etc.). As the dopant level increases, the diffraction peaks arising from the neutral PA decrease smoothly in intensity and, simultaneously, new peaks appear and gradually increase. Neither the original nor the new peaks show measurable shifts in wave vector (q). Finally, at 800 mV only scattering from the doped material is observed. An initial conclusion (consistent with the electrochemical data[5a]) is that doping to 6 mole% Na occurs as a first-order process with coexistence of two separate phases: an ordered doped phase with relatively high Na^+ density together with very lightly doped $(CH)_x$. Data obtained from Durham PA samples are essentially identical to those of Fig. 1. However, because of slight differences[5b] [e.g., the (020) and (110) are not resolved in the neutral Durham material], data from the Durham samples do not show the features of this initial transition as clearly.

Figure 2 contains a series of equatorial scans from a Durham *trans*-$(CH)_x$ sample for Na concentrations from ≈ 7 (828 mV) to ≈ 14 mole% (140 mV). Background corrections have removed scattering arising from the solvent and glass. At 828 mV the main features are two peaks at 1.68 $Å^{-1}$ and 2.92 $Å^{-1}$. Scans at higher q (e.g., in the 607-mV scan) show a third peak at 3.3 $Å^{-1}$. The wave vectors of these three peaks are always in the ratio $1:\sqrt{3}:2$, indicating the continuation of hexagonal symmetry. A triangular lattice is also implied by the disappearance of the (210) reflection (of the monoclinic unit cell of PA; see Fig. 1), and the absence of an equivalent peak in the scattering from the doped material.

Because of the better alignment and the resulting enhanced counting rates, the Durham $(CH)_x$ scans clearly resolve two additional scattering peaks (present but not easily distinguishable in data at similar doping levels for Shirakawa samples). Peaks D and E are first observed at doping levels near 3 mole% (878 mV), initially located at 0.89 and 2.50 $Å^{-1}$. There is also very weak, unresolved scattering around 2.7 $Å^{-1}$ which is present at all doping levels (except in the pristine polymer).

Preliminary scans have been carried out along the c-axis direction. In addition to the (002) of the PA chains, doping-induced scattering appears. For example, at 828 mV, one observes a broad peak centered at 1.27 $Å^{-1}$ consistent with the formation of columns of Na^+ in which neighboring ions are separated (on average) by 4.9 Å with a coherence length of ≈ 25 Å.[6]

As V_{oc} is decreased (increased y) the five peaks identified in Fig. 2 exhibit variations in intensities and shifts in positions. Peaks A, B, and C move to lower q and, regardless of doping level, the ratio of their scattering vectors remains $1:\sqrt{3}:2$; indicative of an expanding triangular lattice. Peaks D and E move to higher q with

D shifting by nearly 10%. No simple model based upon a single slowly varying unit cell can explain the measured shifts. *These continuous changes imply a continuous transformation of the structure.* A similar conclusion was reached by Shacklette and Toth,[5a] but their model assumes a commensurate structure in the a-b plane at the doping levels.

Since peaks A–C (Fig. 2) are relatively intense and vary slowly with increasing y, we attribute them principally to scattering from an average triangular lattice of *trans*-$(CH)_x$ chains. Peaks D and E grow rapidly in intensity and shift with increasing y. At 430 mV an important relationship develops; peaks D and E are located at $\sqrt{3}\times\sqrt{3}$ superlattice positions under the assumption that A, B, and C represent (100), (110), and (200) reflections of the hexagonal PA structure. In addition, if we compare the various scans in Fig. 2, all the scattering peaks are narrowest and best defined at this cell voltage (and associated y). We conclude that at 430 mV, the PA chains and Na columns form a *commensurate superlattice.* A model which includes all of the above features is shown in the inset to Fig. 3(a). The Fourier transform of this structure gives a diffraction profile [solid curve in Fig. 3(a)] in excellent agreement with the data obtained at 430 mV [solid dots in Fig. 3(a)].

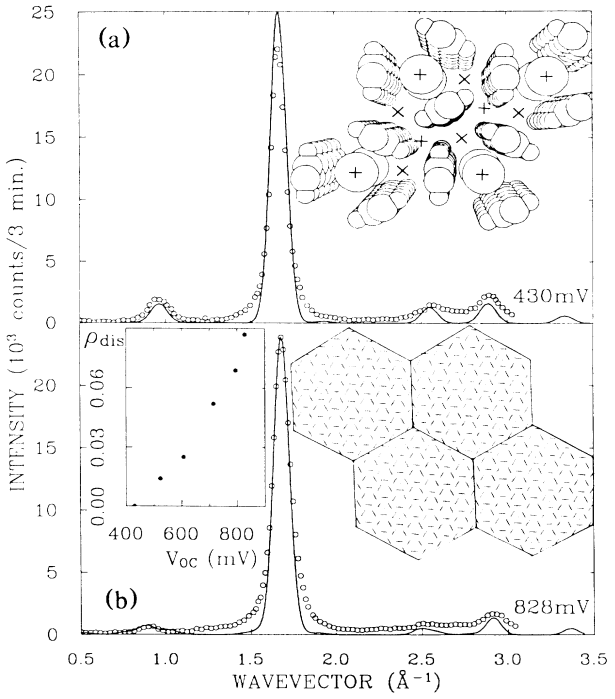

FIG. 3. (a) Comparison between data (circles) and calculated diffraction profile (solid line) for commensurate Na-PA structure (inset). (b) Comparison between data (circles) and calculated diffraction profile (solid line) for discommensurate-domain structure shown in inset (see text). Inset (left): Plot of linear-domain wall density (in inverse PA lattice constant units) vs cell open-circuit voltage.

The 430-mV data lead to a "perfect" channel structure consistent *at this doping level* with the interpretation of the electrochemical voltage spectroscopy data.[5a] This $\sqrt{3}\times\sqrt{3}$ superlattice of Na^+ columns is in reference to a triangular lattice formed by the average spacing between PA chains. The latter is more precisely described as a *modulated* triangular lattice; the centers of the $(CH)_x$ chains are displaced so that the overall hexagonal symmetry is maintained, but with successive chains modulated about the true triangular sites [see inset to Fig. 3(a)]. This model can be extended to incorporate a commensurate-incommensurate transition between the nested PA and Na triangular lattices.

At 828 mV, there is essentially a 10% misfit between the mass-density waves associated with the lattice formed by the PA chains and the Na^+ channels, such that a 3° rotation of the Na lattice results in a large-period commensurability between the two. Because of the strong interactions, we assume that the Na columns are positioned equidistant from nearest-neighbor PA chains, and that the channel structure is maintained locally. This results in a discommensurate structure, shown in Fig. 3(b), right inset, that has locally commensurate regions separated by domain walls which maintain the original PA herring-bone pattern. Thus, the series of scans in Fig. 2 can be understood in terms of an incommensurate regime in which the domains become progressively larger. The linear density of discommensurations (ρ_{dis}) is largest at 828 mV and goes to 0 near 430 mV [see Fig. 3(b), left inset] at which point the system is commensurate and a single-domain $\sqrt{3}\times\sqrt{3}$ superlattice of Na^+ columns forms with respect to the average spacing between PA chains. With this structural model, peak D is a "Na" lattice (100) reflection (obviously there are strong PA contributions to this peak as well) and peak E is principally a first-order modulation satellite resulting from interactions between the Na and Pa lattices. The powder diffraction pattern for this model (not shown) gives an intensity profile in good agreement with the experimental data. The fit can be improved substantially if the model is adjusted slightly to include second-order effects. First, the spacing between the PA chains at the domain walls is less than that of the channel structure in the domains and similar to that of undoped PA. Second, strains which develop at the domain walls result in slight rotations of the domains. The calculated structure factor is shown as the solid curve in Fig. 3(b); it includes rotation of the domains counterclockwise 0.5° and rotation of each channel structure, locally, clockwise 2.5°. The agreement is excellent, implying the essential validity of the model. Moreover, a calculation of the Na concentration at 828 mV, with the use of this domain structure and the Na-Na distance of 4.9 Å within the channel, yields ≈ 7 mole% in agreement with the electrochemical data on

the Durham PA.

Scans at the highest doping levels (227 and 140 mV) indicate a further evolution of the structure. The most notable changes are the rapid radial broadening of the Na (100) peak and the disappearance of peak E, the modulation satellite. On closer inspection, there is also a substantial increase in background intensity at all scan regions above 1.0 $Å^{-1}$. Qualitatively, these features are reminiscent of the scattering results obtained for the commensurate-fluid transition for krypton on graphite.[7] However, the PA peaks shift to lower wave vector, but do not broaden (implying a continued expansion of the PA lattice). Therefore, while the PA lattice remains intact, the Na lattice is unstable at densities higher than the $\sqrt{3}\times\sqrt{3}$ superlattice and transforms into an anisotropic "fluid" within the PA host.

Whereas in graphite, adsorbate or intercalant species tend to occupy the carbon hexagon centers,[7] in PA, the polymer chains themselves can be thought of as occupying the hexagon centers. Thus the preferred sites for the Na dopant columns become hexagon vertices, marked as crosses and plusses in the inset to Fig. 3(b). Our interpretation of this highest-density phase involves disordered occupation of these vertices resulting in a fluidlike structure. We find no evidence of a transformation to the tetragonal structure seen with larger alkalis.[1] Note that the PA lattice parameter increases only slowly within the discommensuration-domain regime (where only ρ_{dis} is changing), but more rapidly at concentrations above that of the $\sqrt{3}\times\sqrt{3}$ superlattice (where random occupancy of "cross" and "plus" sites necessarily expands the lattice). In graphite compounds, the covalently bonded substrate is altered only slightly, while in PA, the average spacing between chains varies considerably and is determined by the Na density.

The information from the structural transitions at doping levels above 6 mole% provides insight into the details of the initial doping transition. With reference to Fig. 1, the (110) and (020) polyacetylene reflections initially change in relative intensity and are gradually replaced by the single peak at 1.685 $Å^{-1}$. Guided by the top-view projections of the a-b plane of the structure of neutral polyacetylene, we propose the following scenario. Injection of the Na ions causes twisting of the polyacetylene chains around the Na ion. This strain changes the setting angle thereby altering the (110) and (020) intensity ratio with minimal changes in lattice spacing. As y increases to about 0.5 mole%, it becomes energetically favorable for the Na ions to condense into nearly homogeneous regions of the discommensuration-domain structure (Na^+ density ≈ 6 mole%) which then coexist with regions of low Na^+ density.

The electronic properties of $[(Na^+)_y(CH)^{-y}]_x$ must be understood in the context of these structural transitions. The spinless charge storage[8] at the most dilute concentrations involves random solitons associated with the Na^+ counterions; the coexistence regime (again, spinless) requires the formation of a soliton lattice. The abrupt first-order increase in the magnetic susceptibility[8] near 6 mole% appears to be the signature of a genuine *electronic* phase transition.[5a] The transition occurs without a corresponding change in structure; only the discommensuration density is varying (and smoothly) in this regime. Finally the decrease in electrical conductivity[5a] observed for sodium-doped PA at ≈ 11 mole% coincides with the transition to the disordered fluid state.

In conclusion, using x-ray scattering carried out *in situ* during electrochemical doping, we have characterized a bizarre sequence of structural transitions. On doping to ≈ 6 mole% there is coexistence between lightly doped regions and a discommensurate-domain channel structure in which commensurate regions are separated by "light" (with respect to Na^+ density) domain walls. Above ≈ 7 mole%, the discommensurate-domain structure fills the entire sample; increasing the Na concentration from ≈ 7 to ≈ 10 mole% is accomplished without a change in structure by our decreasing the density of domain walls. As the discommensuration density falls to zero, the Na channels form a commensurate $\sqrt{3}\times\sqrt{3}$ superlattice with respect to the (average) triangular lattice of polyacetylene chains. At still higher concentrations, the Na lattice becomes unstable and transforms into a disordered fluid phase.

The x-ray scattering studies carried out in Santa Barbara were supported by the Office of Naval Research. Two of us (J.B. and D.C.B.) would like to thank British Petroleum for permission to publish this paper.

[1]R. H. Baughman *et al.*, Mol. Cryst. Liq. Cryst. **118**, 253 (1985).

[2]G. Wieners *et al.*, Makromol. Chem., Rapid Commun. **6**, 425 (1985); J. P. Pouget *et al.*, Mol. Cryst. Liq. Cryst. A **117**, 75 (1985).

[3]J. H. Edwards, W. J. Feast, and D. C. Bott, Polymer **25**, 395 (1984).

[4]H. Shirakawa and S. Ikeda, Synth. Met. **1**, 175 (1980).

[5a]L. W. Shacklette and J. E. Toth, Phys. Rev. B **32**, 5892 (1985).

[5b]D. C. Bott, C. S. Brown, J. N. Winter, and J. Barker, Polymer (to be published). These measurements have revealed small but significant differences in the V vs Q curves for Shirakawa and Durham polyacetylene. We have used the calibrations in Refs. 5a and 5b for the Shirakawa material and the Durham material, respectively.

[6]M. Winokur *et al.*, to be published.

[7]R. J. Birgeneau and P. M. Horn, Science **232**, 329 (1986), and references therein.

[8]F. Moraes, *et al.*, Synth. Met. **11**, 271 (1985).